Computer Assisted Methods in Engineering and Science, **26**: 35–46, 2019, doi: 10.24423/cames.251

IPM 2019

Reconstruction of selected operating parameters of a thermoelectric device

Iwona Nowak[1], Ryszard Buchalik[2], Grzegorz Nowak[2]
Silesian University of Technology
[1] *Institute of Mathematics*
[2] *Institute of Power Engineering and Turbomachinery*
Konarskiego 18A, 44-100 Gliwice, Poland
e-mail: iwona.nowak@polsl.pl

This paper presents preliminary research aimed at recognizing some selected operating parameters of a thermoelectric device. The inverse problem was formulated, for the solution of which a population heuristics (Ant Colony Optimization) was used. In the inverse task, selected parameters important for the cell operation were reconstructed based on relatively easy to obtain temperature measurements within heat exchangers and appropriate measurements of electrical quantities. The heuristics used, reconstructs the estimated variables, minimizing the differences between data from the measurements and data calculated in the model for their determined values. Since inverse tasks, as ill-conditioned problems, are characterized by high sensitivity to measurement errors, the tests began with calculations based on numerically generated data in order to fully maintain control of their disturbances.

Keywords: thermoelectricity, heat transfer, complex thermal system, thermal resistance, condition tracking, condition optimization, inverse problem, sensitivity analysis, ant colony optimization.

Nomenclature

I	–	electric current [A],
$\mathbf{J} = \mathbf{J}_f$	–	Jacobian matrix,
K	–	thermal conductivity [W/K],
P	–	power [W],
R	–	electric resistance [Ω],
Q	–	heat flux [W/m^2],
T	–	temperature [K],
$\mathbf{W}$	–	covariance matrix,
V	–	voltage [V],
$\mathbf{X}$	–	vector of estimated parameters,
$\mathbf{Y}$	–	vector of measure quantities,
$\delta\mathbf{Y}$	–	absolute error of reconstruction [%],
Z	–	sensitivity coefficient,
k	–	number of pheromone stains,
r	–	resistance [K/W].

Greek symbols

α – Seebeck coefficient [V/K],
η – efficiency,
Φ – objective function,
σ – standard deviation
μ – expected value.

Subscripts and superscripts

0 – initial,
eqv – equivalent,
c – cold side of thermoelectric module,
ca – constant temperature (cold side) heat source,
int – internal,
cond – conductive,
conv – convective,
h – hot side of thermoelectric module,
ha – constant temperature (hot side) heat source,
m – measured,
opt – optimal,
sc – short circuit.

1. Introduction

In many engineering problems determination of true parameters characterizing object under investigation is crucial because it allows modelling its behaviour and assessment of its quality. Such a situation occurs in the case of thermoelectric generators where not only the thermoelectric module affects the performance but also the co-working heat exchangers [3, 4].

The aim of the paper is to discuss the possibility of formulating an inverse problem and using its solution to study thermoelectric elements operating on the basis of the Seebeck effect, which is the electromotive force generation on a junction of two different materials whose ends are the kept at different temperatures. It usually consists of two "legs" of different semiconductors connected at one (hot) end and disconnected (open circuit) at the other (cold). The voltage generated depends on the Seebeck coefficient (material-in-contact dependent) and the temperature difference between junctions:

$$V = \alpha \cdot \Delta T. \tag{1}$$

Since a single junction is able to generate a tiny magnitude of electromotive force, a lot of legs are connected in series to produce output voltage.

The "legs" are covered with an electric insulator, usually ceramic plates, which separate them from the ambient (heat source and heat sink).

Thermogenerators (TEGs) enable the direct conversion of thermal energy into electricity. As they have no moving parts, they are extremely durable and are therefore suitable for the production of auxiliary electrical energy in thermal systems.

In this type of devices, the source of heat used to generate electricity can be both the heat flux directed to the device and waste heat. In the latter case it will increase the overall energy efficiency of the system.

Determination of TEG operation characteristics requires the design of an appropriate test rig providing full information on the amount of energy supplied and derived from the system (thermal

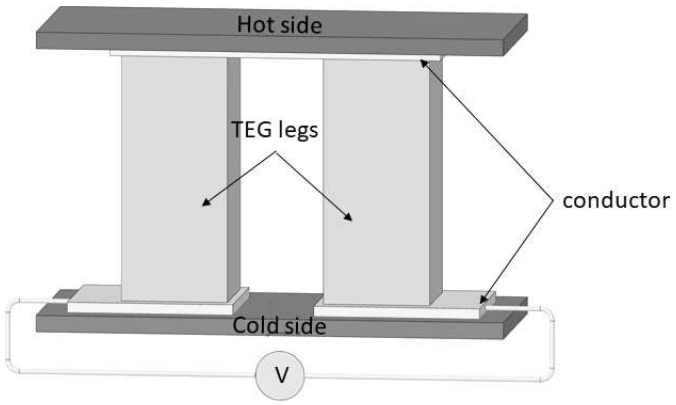

Fig. 1. Thermoelectric cell.

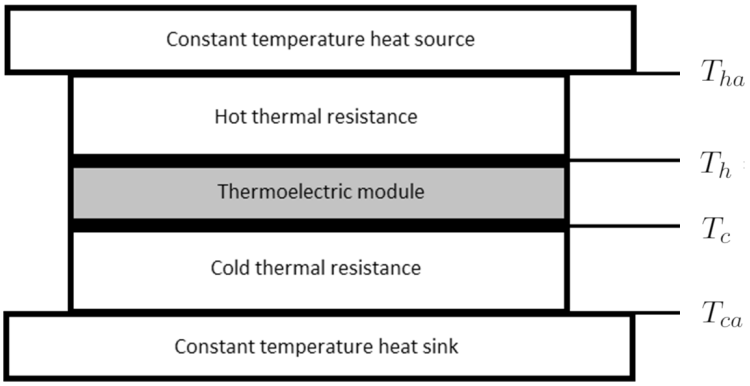

Fig. 2. Schematic diagram of a thermoelectric set.

and electrical). The next element is the best possible determination of thermo-electric parameters of the module and identification of thermal resistance and electrical resistance. Some of these quantities are relatively straightforward to measure (electrical values), whereas we can say very little about the others – measurement is indirect and burdened with errors. These are, first of all, unknown material parameters of cell components (conductivity coefficients, thermal capacity, cell filling density, Seebeck coefficient, etc.), contact resistances on the surface and inside the cell. Most importantly – it is nearly impossible to measure a temperature of the thermoelectric joint for assembled TEG. Usually, the temperature in the thermoelectric system is measured at some distance, so its value is slightly different. This phenomenon influences the generated electromotive force (1) and overall operating parameters. It is possible to get rough approximation assuming that measured temperature is a true temperature of thermoelectric joint. Although this assumption leads to some miscalculations, and also it cannot be used in a condition where additional thermal resistance is significantly large, e.g., inappropriate clamping force, lack of or dried thermal grease, etc.

The main idea behind this paper is a question – is it possible to find true parameters of the thermoelectric cell (Seebeck coefficient, internal resistance, thermal conductivity) and predict the cell's behaviour in various working condition (electrical and thermal)? The answers can also indicate the influence of auxiliary equipment (e.g., heat exchanger) and evaluate the potential of thermoelectric system improvement by its modification.

2. Problem formulation and modelling

Determination and description of possible variants of laboratory testing is important for identification of the properties of the thermoelectric cell and/or the entire system in which it is installed.

Conventional testing of this type of devices requires a large number of measurement devices, measurement points and long measurement time. It is hypothesized that this process can be significantly simplified by measuring selected parameters at arbitrary working points. Such an approach would not only simplify the experiment itself but also reduce the number of potential sources of measurement errors.

Solution of a properly formulated inverse problem seems to give a chance to reproduce very difficult, practically impossible to determine in a direct way parameters (temperature of contacts inside the device, thermal capacity of individual elements), and, most importantly, to predict the behaviour of the system at any operating conditions, based on a few measurements only.

In this study, the model of a system containing a thermoelectric cell is considered [2]. The most important parts of the model are thermoelectric cell, heat exchangers and constant temperature heat sources. The main idea behind this approach is to implement the influence of finite thermal resistance between constant temperature heat source, thermoelectric joints in the cell and temperature measurement points. Thermoelectric cell often consists of some ceramic coating that has a thermal resistance. Conduction in heat exchanger is also characterized by some thermal resistance. Contact layer between this heat exchanger and thermoelectric cell has some thermal resistance too, and this one is the hardest to predict in analytical way because it depends on thermal grease quality, its physical and chemical properties, surface smoothness (finishing) and clamping force (very strong influence). It can also be a subject to change in long time period. Thermal resistance was assumed to be constant, so the ratio of a temperature difference across all elements (and each individual one) (between thermoelectric joint and the constant temperature heat) source is constant. The result of this assumption is that measured temperature differs from real joint temperature by a value proportional to the heat flux. Heat flux conducted through the thermoelectric module is a result of not only simple conducting, but also thermoelectric phenomena occurring on each side of the thermoelectric cell (each joint) (Peltier effect). This modifies the heat flux and as a result, the temperature distribution, which influence the performance of the thermoelectric system. Obviously, the electric current and electrical resistance of the power receiver correspond to optimal (max power or max efficiency) working condition changes.

The overall efficiency of the thermoelectric system (2) in the case considered is a ratio of an electric power produced and the heat flux entering into the system. Electrical power can be easily determined and measured with relatively high accuracy. This results from electric current in the circuit and voltage generated at the output of the thermoelectric cell. The amount of heat flux entering the system is mainly a consequence of three phenomena. Cell materials have a finite thermal conductivity, which results in simple conduction of heat ($Q_{\text{Conduction}}$). Secondly, they have some finite electrical resistance, so electric current flow is a source of Joule heat (Q_{Joule}). Finally, since a thermoelectric joint exists, when the electric current is imposed upon the system, it absorbs or generates some amount of heat dependent on its temperature (Peltier effect).

$$\eta = \frac{P}{Q_h} = \frac{V \cdot I}{Q_{\text{Peltier}} + Q_{\text{Conduction}} + Q_{\text{Joule}}}, \tag{2}$$

where P – the output power (useful effect) of the thermoelectric module and Q_h – the total heat flux supplied to entering the thermoelectric module.

If we expand the heat fluxes:

$$\eta = \frac{(\alpha \cdot \Delta T - I R_{\text{int}}) \cdot I}{\alpha_{\text{eqv}} I T_h + K_{\text{eqv}} \Delta T - \frac{1}{2} I^2 R_{\text{int}}}. \tag{3}$$

To make use of the above relation, quantities characterizing thermoelectric cell itself have to be involved in this description (3). Useful voltage results from the electromotive force generated minus voltage drop at internal resistance. Electromotive force is a product of temperature difference at thermoelectric joints and the Seebeck coefficient. Here, the Seebeck coefficient is understood as an

equivalent one for the entire cell, which means it involves the Seebeck coefficient for material connections in the core of the cell and also their amount, arrangement and electrical connection between them (serial connection multiplies the electromotive force). Voltage drop at internal resistance is proportional to its value and electric current in the circuit. Parameter K_{eqv} denotes a quantity which describes simple conduction of heat, without considering thermoelectric phenomenon. Its value results from thermal conductivity of used materials and geometrical arrangement of the cell. In this approach it is a proportionality coefficient between thermal difference and heat conducted without electric current in the circuit. This amount of heat is increased by the Peltier effect. It results from power absorbed at hot side of thermoelectric joints [8]. This power is a product of current and voltage at these joints. This voltage can be expressed as the multiplication of the Seebeck coefficient and absolute temperature of these joints, and this is known as the Peltier coefficient. Electric current flowing in a circuit, due to internal resistance, creates voltage equal to electric current multiplied by internal resistance, this voltage multiplied by electric current gives the amount of the Joule heat [7]. Half of this heat is expelled at the hot side, which diminishes the overall amount of heat due to the superposition.

The relation between the constant temperature heat source or heat sink and the temperature of the thermoelectric module surface can be expressed in the following way for conduction (4), (5):

$$T_c = T_{ca} + Q_c \cdot r_c, \tag{4}$$

$$T_h = T_{ha} - Q_{(\text{conv})h} \cdot r_h. \tag{5}$$

The temperature of the thermoelectric joints, at the hot and cold side, which is considered as a true temperature of the cell can be expressed based on the above described assumptions. The thermal resistance of heat exchangers at the hot side (denoted by r) is a ratio of the temperature drop across this heat exchanger and the heat flux. So, the true temperature of the cell's hot side is the temperature of the hot heat source (T_{ha}) diminished by thermal resistance multiplied by heat flux.

This modification is a source of complication because the heat flux modifies the temperature of the cell and in consequence modifies the optimal condition characteristic and finally the heat flux. The system becomes complex and the analytical solution is hard to obtain.

In the above relationships, all of the crucial coefficients are assumed constant in working conditions under investigations and their significant vicinity.

3. Measurements

In order to determine the performance characteristics of the thermoelectric system, a test rig was built. It consisted of two $10 \times 10 \times 4$ cm copper blocks and a thermoelectric cell clamped between them. One of the blocks consisted of five electric heaters (heat source), while the other had five cooling channels (heat sink) through which cooling water passed by. The true temperature of the assembled thermoelectric module is nearly impossible to measure directly. So the temperatures of selected points in the middle of each copper block were taken as measured temperatures and were maintained at a constant level by an electric heater and cooling water stream, both controlled by PID regulators. Those points are equivalent of the constant temperature heat source. In this case, in a steady-state condition. Steady-state benchmarks of the cell were performed.

To gain additional information about the thermal resistance between constant temperature heat source and the thermoelectric cell, rapid-state tests were performed. The crucial remark, in this case, is that electrical parameters, in this case, the value of electric current in the thermoelectric module circuit, can change very fast (a few microseconds). Changes of temperature distribution occur significantly slower. This situation allows determination of operational parameters (especially output voltage, electromotive force and circuit) for any possible value of current (between short circuit and open circuit) for every achievable temperature of the thermoelectric module (thermoelectric joints) in steady-state conditions. As it was mentioned above, change in electric current

causes a change in temperature of the thermoelectric module due to a change in heat flux and the presence of r. However, this change in temperature occurs significantly slower. So, for a few milliseconds after the change of electric current observation is made for a state corresponding to the "old" temperatures, which was present before the change in the electric current, and "new" electric current voltage.

In Fig. 3, an exemplary result of this kind of measurement is presented. The process was started at steady-state open circuit condition, and then the short circuit was applied by turning on a fast electrical switch. The value of current jumps up and slowly moves slightly down into a steady-state value within about 3 sec. The peak value must be read in a few milliseconds, in this time range the changes occur mildly. Applying the short circuit increases the Peltier effect, thus increasing the heat flux entering the cell, and in consequence enlarging the temperature drop (between the heat source and thermoelectric cell). So, the temperature gradient at the thermoelectric module becomes smaller, which results in a smaller electromotive force and smaller current. The peak value from rapid state measurement corresponds to higher temperature difference, present in the open-circuit state. Analogous situation can occur in the opposite situation when performing the rapid state measurement from the steady-state short circuit to the open circuit. In this case, a voltage does not increase instantly to the steady-state open circuit, but to a slightly smaller value, corresponding to the temperature gradient for steady-state short circuit (smaller temperature gradient).

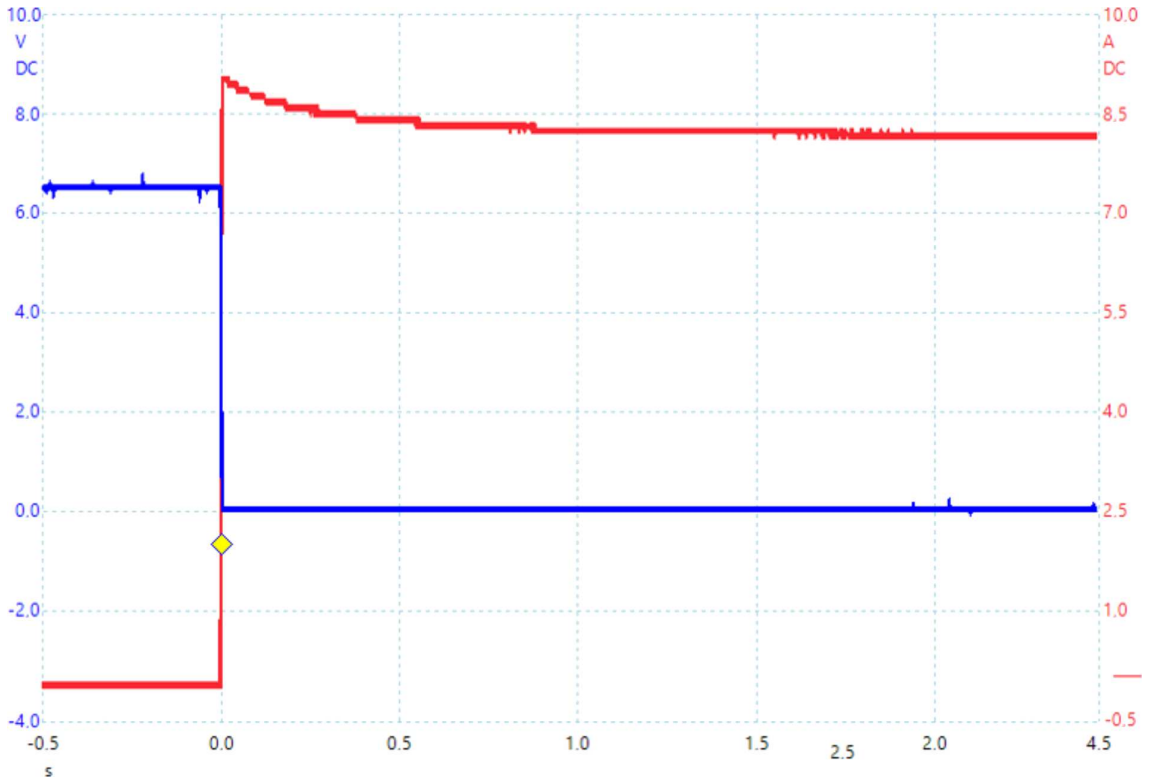

Fig. 3. Variation of voltage (blue) and current (red) in the moment of short circuit.

In Fig. 4, those measurements are shown. Green and red dots denote values from rapid state measurements for both situations described, respectively. A slope of these lines results from internal resistance of the cell and it is its direct representation. Blue dots represent steady-state measurements. A difference of this value (rapid peak and steady state) clearly shows the existence of postulated thermal resistance r. If r would be zero (no resistance) the peak and steady state would be equal (rectangular shape of the current diagram in Fig. 3). Assuming steadiness of mentioned coefficients, the ratio of peak voltage to steady-state voltage and the peak current to steady-state

current is equal (the same slope). This quantity has been introduced to the proposed model and is presented as the equation:

$$\frac{I_0}{I_{sc}} = \frac{T_0 - T_{ca}}{T_{I_{sc}} - T_{ca}}. \tag{6}$$

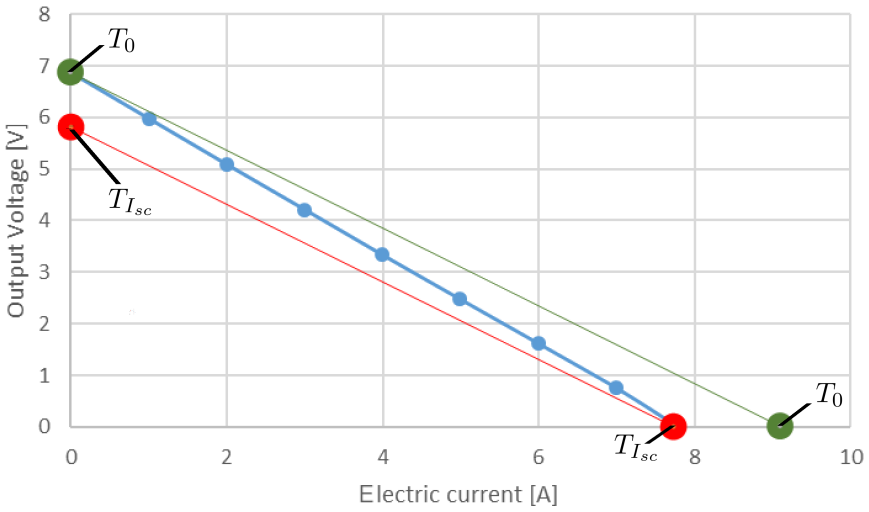

Fig. 4. Idea of proposed measurement method. Blue dots represent steady-state conditions. Red and green lines represent Rapid-state measurements.

Although in the presented work, it was assumed that the tests would be conducted on a numerical example, the technical possibilities of obtaining measurements in real conditions were the basic guidelines to determine which parameters can be data and which must be reproduced. The results presented in the next part serve as a preliminary assessment of whether future results (based on real measurements) can be treated as reliable.

4. Inverse problem formulation

As it was mentioned in Sec. 2, the mathematical model, in the direct approach allows determination values of I_{sc}, I_0, q_{T_0} and q_{sc} based on heat resistance r, equivalent thermal conductivity K_{eqv} and equivalent Seebeck coefficient α_{eqv}. Because these quantities are difficult or impossible to measure, we suggest to designate them in the inverse procedure based on I_{sc}, I_0, q_{T_0} and q_{sc} measurements, which can be obtained with relatively good accuracy according to Sec. 3.

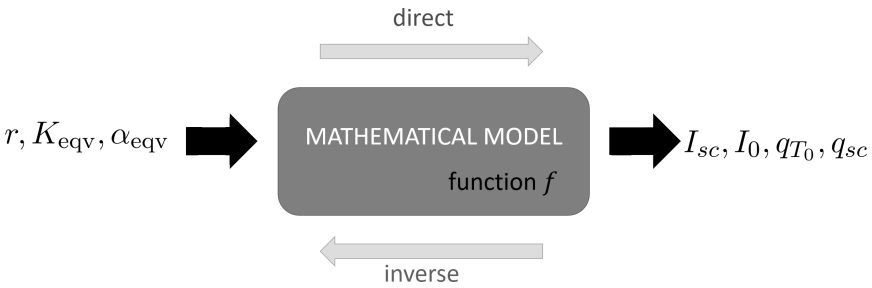

Fig. 5. Scheme of direct and inverse formulation.

For this purpose, the inverse problem is formulated as the problem of minimization of the objective function Φ in the form:

$$\Phi(\mathbf{X}) = \|\mathbf{Y} - \mathbf{Y}_m\| = (\mathbf{Y} - \mathbf{Y}_m)^T(\mathbf{Y} - \mathbf{Y}_m) = \sum_{i=1}^{4}\left(y_i - y_i^{(m)}\right)^2 \tag{7}$$

or alternatively, if the covariance matrix $\mathbf{W}$ is available:

$$\Phi(\mathbf{X}) = \|\mathbf{Y} - \mathbf{Y}_m\| = (\mathbf{Y} - \mathbf{Y}_m)^T\mathbf{W}^{-1}(\mathbf{Y} - \mathbf{Y}_m). \tag{8}$$

In the above formulas, we assume that $\mathbf{X} = [r, K_{\text{eqv}}, \alpha_{\text{eqv}}]$, $\mathbf{Y} = [I_{sc}, I_0, q_{T_0}, q_{sc}]$ while $\mathbf{Y}_m$ is a vector of measurements used to solve the inverse problem.

Because we aim to determine whether it is possible to reconstruct $\mathbf{X}$ parameters based on the data $\mathbf{Y}_m$ read at the test stand, the procedures proposed were tested on a numerical experiment designed for this purpose. All calculations were conducted with measurement data generated numerically (without disturbance and with a pseudo-randomly generated disturbance with normal distribution). This approach is typical of early research convention because it gives the opportunity to assess how the developed approach deals with the solution of the inverse problem while the disturbances coming from real measurements are eliminated.

Two approaches were tested. The first one was based on the sensitivity analysis (SA) using the iterative process, which is necessary due to the non-linear nature of the direct problem. In the second approach, the Real Ant Colony Optimization was used, in which the heuristics determine the values of estimated parameters on the basis of minimizing the difference between the measurements and the model response.

4.1. Sensitivity analysis approach

Generally, SA is an approach that is based on determining the influence of individual variables on the values and/or parameters of a function [1, 6, 10]. This influence is determined on the basis of the sensitivity coefficients defined as a derivative of the j-th value of a function with respect to i-th estimated variable

$$Z_{ij} = \frac{\partial y_i}{\partial x_j}.$$

The sensitivity coefficient may be determined numerically and/or analytically, which depends on the specificity of the problem.

If the mathematical model is treated as a multivariable vector-valued function $f: D \to \mathbb{R}^4$, $D \subseteq \mathbb{R}^3$, $f(\mathbf{X}) = \mathbf{Y}$ then in the neighborhood of the arbitrary point $(\mathbf{X}_0, \mathbf{Y}_0 = f(\mathbf{X}_0))$ it can be expanded into the Taylor series.

The first two terms of the Taylor expansion, written in vector form, lead to the following dependence:

$$\mathbf{Y} \approx \mathbf{Y}_0 + \mathbf{J}_f(\mathbf{X}) \cdot (\mathbf{X} - \mathbf{X}_0), \tag{9}$$

where $\mathbf{J}_f$ is the Jacobian matrix over the vector-valued function f defined by:

$$\mathbf{J}_f(\mathbf{X}) = \frac{d}{d\mathbf{X}} f(\mathbf{X}) = \begin{bmatrix} \dfrac{\partial y_1}{\partial x_1} & \cdots & \dfrac{\partial y_1}{\partial x_4} \\ \vdots & \ddots & \vdots \\ \dfrac{\partial y_1}{\partial x_1} & \cdots & \dfrac{\partial y_1}{\partial x_4} \end{bmatrix}.$$

It is easy to notice that matrix $\mathbf{J}_f$ collects sensitivity coefficients.

By inserting the expression (9) into the objective function (7), it is possible to show that the function Φ reaches the minimum when[1]:

$$\mathbf{X}_{\min} \approx \mathbf{X}_0 + \left(\mathbf{J}^T\mathbf{J}\right)^{-1}\mathbf{J}^T\left(\mathbf{Y}_m - \mathbf{Y}_0\right) \tag{10}$$

or in the case of functions (8) for:

$$\mathbf{X}_{\min} \approx \mathbf{X}_0 + \left(\mathbf{J}^T\mathbf{W}^{-1}\mathbf{J}\right)^{-1}\mathbf{J}^T\mathbf{W}^{-1}\left(\mathbf{Y}_m - \mathbf{Y}_0\right). \tag{11}$$

Note that the product on the right-hand side of the equations gives, *de facto*, information on how much the point $\mathbf{X}_0$ should be "moved" to get the optimal solution. Note that this factor is a multiplier of the linear difference $\mathbf{Y}_m$ and $\mathbf{Y}_0$. The solutions obtained according to (10) or (11) will only make sense in linear problems or with very small differences of $\mathbf{Y}_m$ and $\mathbf{Y}_0$.

The problem presented is not a linear one, therefore using the formulas (10) or (11) would be useless. In the case of non-linear models, however, it is possible to perform calculations in the iterative process, in which the "offset" of the known $\mathbf{X}_0$ towards the solution is done only by a fraction of the value indicated by (10) or (11).

Therefore, we define further approximations of the solution as:

$$\mathbf{X}^{(i)} \approx \mathbf{X}^{(i-1)} + \varepsilon \cdot \left(\mathbf{J}^T\mathbf{J}\right)^{-1}\mathbf{J}^T\left(\mathbf{Y}_m - \mathbf{Y}^{(i-1)}\right) \tag{12}$$

or

$$\mathbf{X}^{(i)} \approx \mathbf{X}^{(i-1)} + \varepsilon \cdot \left(\mathbf{J}^T\mathbf{W}^{-1}\mathbf{J}\right)^{-1}\mathbf{J}^T\mathbf{W}^{-1}\left(\mathbf{Y}_m - \mathbf{Y}^{(i-1)}\right), \tag{13}$$

where ε is a coefficient determining the degree of displacement in a single iteration. We assume that $\mathbf{X}^{(0)} = \mathbf{X}_0$, and the iterative process is carried out until the difference $\mathbf{Y}_m - \mathbf{Y}^{(i)}$ is satisfyingly small.

4.2. Ant colony optimization

The Real Ant Colony Optimization (RACO), originally proposed by Dorigo and Birattari in [5], is the heuristics inspired by the behaviour of ant colonies. The idea of this method is based on the formation of so-called pheromone stains (possible solutions) of increasing intensity, which are produced by artificial ants.

The optimization procedure starts with generating the so-called initial archive of k pheromone "stains" (solutions) which are arranged with respect to their quality (identical with values of the objective function). Then, in the iteration procedure, new and mostly better solutions are the results of ants' work, where each of them imposes a new pheromone stain. The ants actions are controlled by an appropriate probabilistic model, which is realized by random selection by each ant of a j-th solution (stain of pheromone in the existing archive) with probability

$$p_j = \frac{\omega_j}{\sum\limits_{l=1}^{k}\omega_l}, \tag{14}$$

where ω_j is weight connected with j solution determined with Gaussian $g(\mu,\rho) = g(1,k)$ (k – number of stains), i.e.,

$$\omega_j = \frac{1}{k\sqrt{2\pi}} \cdot e^{\frac{-(j-1)^2}{2k^2}}. \tag{15}$$

[1]For the sake of simplicity, a notation $\mathbf{J}_f(\mathbf{X}) = \mathbf{J}$ is used.

The ants prefer to choose a seat/track more saturated with pheromones, and that is why the weights reflect the pheromone "intensity", which is associated with solution quality. Using the function (15) ensures that the weights ω_j have only positive values, which is important in determining the values p_j according to formula (14).

In the next step, the ants sample the subspace in the surroundings of selected stain (represented by vector $\mathbf{s}_j = (s_j^1, s_j^2, \cdots, s_j^l)$) applying a pheromone trail with random Gaussian distribution. The probability that r-th component of a newly imposed stain occurs at x is determined by the following formula:

$$p(x) = g(x, \mu, \sigma) = \frac{1}{\sigma\sqrt{2\pi}} e^{\frac{-(x-\mu)^2}{2\sigma^2}}, \tag{16}$$

where the expected value $\mu = s_j^r$ is related to the position of the stain selected by an ant, while the standard deviation $\sigma = \xi \sum_{p=1}^{k} \frac{|s_p^r - s_j^r|}{k-1}$ is the average distance between the r-th component of the selected stain and the others within the population. Construction is repeated for each of m ants (m new pheromone "stains" are obtained). Using the Gaussian function enables the new solutions to be produced in regions that are found promising.

The heuristics described above turns out to be a very efficient method of optimization, also in engineering problems [9]. Although, optimization is carried out in the iterative process (typical for heuristics), using the probabilistic approach to search the solution space is often more efficient than in GA.

For the above reasons, choosing RACO to solve the inverse problem considered in this work seems to be justified.

5. Numerical results

In the direct model, the following fixed physical parameters were adopted: temperature of the heat source and the heat sink $T_{ha} = 1\,147$ K, $T_{ca} = 303$ K, internal electric resistance $R_{\text{int}} = 2.58\ \Omega$, and a contact surface area $A = 62 \times 62$ mm^2. In order to generate data, the values of parameters, the reconstruction of which is a goal in the inverse formulation, were also adopted: heat resistance of selected elements $r = 1.5$ K/W, equivalent thermal conductivity $K_{\text{eqv}} = 1.4$ W/K, and equivalent Seebeck coefficient $\alpha_{\text{eqv}} = 0.025$ V/K. In the inverse problem, these values will be the reference values collected in a vector $\mathbf{Y}_{\text{exact}}$.

For the parameter values set, in the direct model, the values I_{sc}, I_0, q_{T_0} and q_{sc} were determined and burdened with pseudo-random errors. Then they were treated as measurement data $\mathbf{Y}_m$ for the inverse problem procedure.

5.1. Reconstruction on the basis of undisturbed data

In the first approach, the inverse problem was solved for undisturbed data.

An attempt was made to reproduce the reference values using SA and RACO, which would help assessing whether the selected procedures are suitable for solving the problem. As a condition for the iterative process termination, it was assumed that $\Phi(\mathbf{X}_{\text{opt}}) < 10^{-5}$.

According to (12) or (13), the use of SA requires a preliminary estimation of the reconstructed variables. Assuming $\mathbf{Y}_0 = (3.0, 0.7, 0.045)$ and $\varepsilon = 0.05$ after just 38 iterations a solution $\mathbf{Y}_{\text{opt}} = (1.5044, 0.4014, 0.02308)$ was obtained. Such a result translates into absolute errors $\delta\mathbf{Y}_{\text{opt}} = (0.29\%, 0.35\%, 0.35\%)$.

In the procedure based on RACO, no more than 30 iterations were required to obtain an acceptable result, which due to the nature of the procedure was equivalent to 150 evaluations of the

objective function[2]. The result obtained is $\mathbf{Y}_{\text{opt}} = (1.531209, 0.42354, 0.02326)$ which means the error vector equals $\delta\mathbf{Y}_{\text{opt}} = (0.8\%, 0.98\%, 1.13\%)$.

Runs of both iterative processes are shown in Fig. 6.

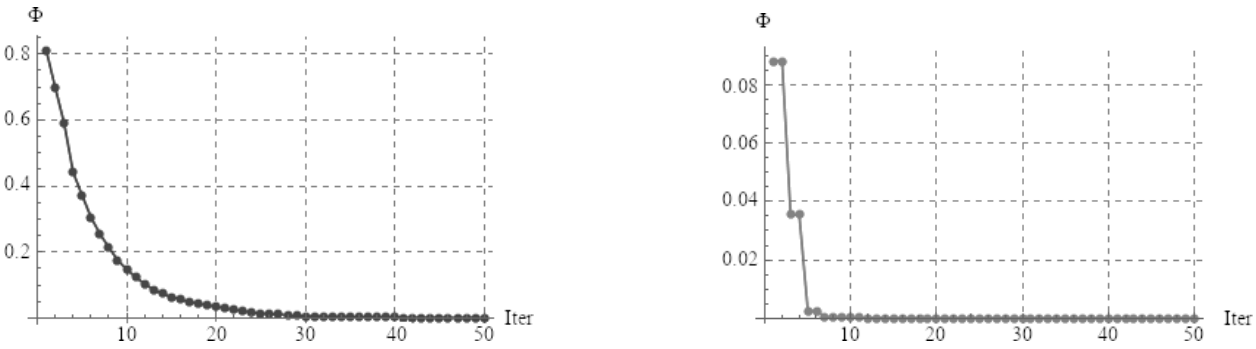

Fig. 6. The course of the iterative process in the case of SA (left chart) and ACO (right chart) for undisturbed data.

It is clearly seen, the first test showed the small advantage of SA, which in the conditions of the first task turned out to be more accurate than RACO. The second method is also a bit more efficient (similar accuracy with lower computing effort).

5.2. Reconstruction on the basis of disturbed data

The greatest difficulties in solving inverse problems result from the ill-conditioned nature of the problem. For this reason, it is extremely important to assess how the proposed solving procedures deal with error-affected data and to what extent these errors are transferred to the result of the inverse task.

In the second example, the disturbed data was obtained by adding to the direct solution $\mathbf{Y}_m$ the pseudo-random errors (with normal distribution). It was assumed that the maximum error (i.e., 3σ) does not exceed $\delta\mathbf{Y}_m = \{1\%, 2\%, 5\%, 5\%\}$.

As in the previous example, both RACO and SA were used in the calculations.

The use of RACO, in this case, gave $\mathbf{Y}^{ev}_{\text{opt}} = (1.45225, 0.37692, 0.02175)$ as the average result in 10 different runs (with errors $\delta\mathbf{Y}^{ev}_{\text{opt}} = (3.1\%, 6.1\%, 5.8\%)$). It should be noted at the same time that the best result obtained is $\mathbf{Y}_{\text{opt}} = (1.50229, 0.408868, 0.023421)$ with $\delta\mathbf{Y}_{\text{opt}} = (0.12\%, 2.17\%, 1.8\%)$.

In reconstructions on the basis of disturbed data using only SA, some instabilities in the convergence appeared often (left chart in Fig. 7). Although it was not possible to clearly determine what was the reason, quite often in the second approach it was decided to conduct the process in two stages: first performing 10 steps RACO (which required 50 evaluations), and the found solution to be used as $\mathbf{Y}_0$ to a procedure based on sensitivity analysis. In this modified procedure, the 1st step is responsible for exploring the space, generating the initial estimation of the solution, while the 2nd step is the operation, whose main goal is to increase the accuracy of the solution. Such an approach, apart from eliminating the problem of instability, reduced the number of necessary evaluations of the objective function and, consequently, the calculation time. The average result obtained in this way is $\{1.59779, 0.430064, 0.0255501\}$ and the course of the 2nd step is presented in the right chart in Fig. 7.

[2]In ACO procedure five pheromone stains were used, what equals the number of function evaluations in a single iteration.

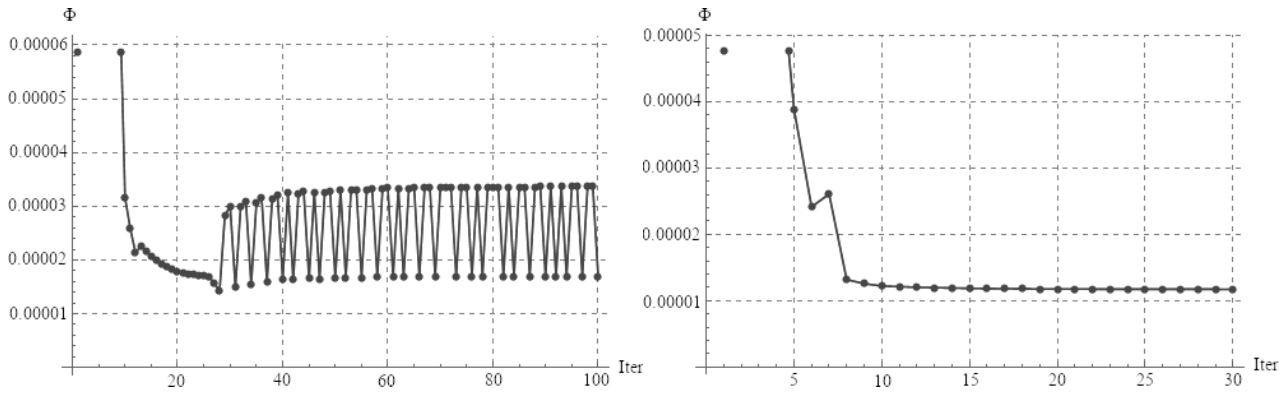

Fig. 7. The course of the iterative process in the case of SA (left chart) and the SA-RACO combined approach (right chart) for undisturbed data.

6. Summary

Numerical tests carried out for the needs of this work allowed to formulate some useful conclusions for future research.

- If the quality of measurements is good, the method based on SA (or two steps procedure) is more efficient than the use of only heuristic ACO.
- For unstable computational process, it is recommended to use heuristics (if possible several runs) and its statistical treatment could be a remedy.
- It was observed that sensitivity coefficients are of significantly various ranges, which leads to unstable solutions for some sets of measurements.
- Good results are achieved by combining the proposed methods, ACO for preliminary determination of the estimated values and SA as a type of local search in order to increase accuracy.

The gained experience will be used for actual problems with TEM measurements planned in the near future.

Calculations were mainly done in the in-home programs (in Fortran) created for work purposes. Other calculations and graphics were created with Wolfram Mathematica.

References

[1] R.C. Aster, B. Borchers, C.H. Thurber. *Parameter estimation and inverse problems*. Elsevier, 2019.
[2] R. Buchalik, I. Nowak, K. Rogoziński, G. Nowak. Detailed model of a thermoelectric generator performance. *Journal of Energy Resources Technology*, 1–12 (12 pages), Paper No.: JERT-18-1924, 2019 (in press).
[3] M. Chen, S.S. Lu, B. Liao. On the figure of merit of thermoelectric generators. *Journal of Energy Resources Technology*, **127**(1): 37–41, 2005.
[4] L. Chen, J. Gong, F. Sun, C. Wu. Effect of heat transfer on the performance of thermoelectric generators. *International Journal of Thermal Sciences*, **41**(1): 95–99, 2002.
[5] M. Dorigo, M. Birattari. *Ant colony optimization*. Springer US, 2010.
[6] M. Kern. *Numerical methods for inverse problems*. ISTE and John Wiley & Sons, 2016.
[7] H. Lee, J. Sharp, D. Stokes, M. Pearson, S. Priya. Modeling and analysis of the effect of thermal losses on thermoelectric generator performance using effective properties. *Applied Energy*, **211**: 987–996, 2018.
[8] G.S. Nolas, J. Sharp, H.J. Goldsmid. *Thermoelectrics: Basic principles and new materials developments*. Springer-Verlag Berlin Heidelberg New York, 2001.
[9] I. Nowak. Heuristics applying stochastic information as tools for thermoacoustic standing-wave engine optimization. *CAMES*, **25**(1): 3–19, 2018.
[10] H.W. Engl, M. Hanke, A. Neubauer. *Regularization of inverse problems*. Vol. 375. Springer Science & Business Media, 1996.